Next generation restoration metrics: using soil eDNA bacterial community data to measure trajectories towards rehabilitation targets

Article

Accepted Version

It is advisable to refer to the publisher's version if you intend to cite from the work. See Guidance on citing.

www.reading.ac.uk/centaur

CentAUR

Central Archive at the University of Reading

Reading's research outputs online

1 **Next generation restoration metrics: Using soil eDNA bacterial community data to**

2 **measure trajectories towards rehabilitation targets**

3

4 **Author details:**

5 Craig Liddicoat[1,2], Siegfried L. Krauss[3,4], Andrew Bissett[5], Ryan J. Borrett[6], Luisa C.

6 Ducki[1,6], Shawn D. Peddle[1], Paul Bullock[7], Mark P. Dobrowolski[4,8,9], Andrew Grigg[10], Mark

7 Tibbett[4,11], Martin F. Breed[1]

8

9 [1]College of Science and Engineering, Flinders University, Adelaide, Australia

10 [2]School of Public Health, The University of Adelaide, Adelaide, Australia

11 [3]Kings Park Science, Western Australia Department of Biodiversity Conservation and Attractions,

12 Perth, Australia.

13 [4]School of Biological Sciences, University of Western Australia, Perth, Australia

14 [5]CSIRO Oceans and Atmosphere, Hobart, Australia

15 [6]College of Science, Health, Engineering and Education, Murdoch University, Perth, Australia

16 [7]South32 Worsley Alumina, Perth, Australia

17 [8]Iluka Resources Limited, Perth, Australia

18 [9]Harry Butler Institute, Murdoch University, Perth, Australia

19 [10]Alcoa of Australia Limited, Perth, Australia

20 [11]Department of Sustainable Land Management & Soil Research Centre, School of Agriculture,

21 Policy and Development, University of Reading, Berkshire, United Kingdom

22

23

24 **Corresponding author:**

25 Craig Liddicoat, College of Science and Engineering, Flinders University, Sturt Road

26 Bedford Park SA 5042, Adelaide, Australia

27 E-mail address: craig.liddicoat@flinders.edu.au

28

29

30   **Next generation restoration metrics: Using soil eDNA bacterial community data to**

31   **measure trajectories towards rehabilitation targets**

32

33   **Abstract**

34   In post-mining rehabilitation, successful mine closure planning requires specific, measurable,

35   achievable, relevant and time-bound (SMART) completion criteria, such as returning

36   ecological communities to match a target level of similarity to reference sites. Soil microbiota

37   are fundamentally linked to the restoration of degraded ecosystems, helping to underpin

38   ecological functions and plant communities. High-throughput sequencing of soil eDNA to

39   characterise these communities offers promise to help monitor and predict ecological

40   progress towards reference states. Here we demonstrate a novel methodology for monitoring

41   and evaluating ecological restoration using three long-term (> 25 year) case study post-

42   mining rehabilitation soil eDNA-based bacterial community datasets. Specifically, we

43   developed rehabilitation trajectory assessments based on similarity to reference data from

44   restoration chronosequence datasets. Recognising that numerous alternative options for

45   microbiota data processing have potential to influence these assessments, we

46   comprehensively examined the influence of standard versus compositional data analyses,

47   different ecological distance measures, sequence grouping approaches, eliminating rare taxa,

48   and the potential for excessive spatial autocorrelation to impact on results. Our approach

49   reduces the complexity of information that often overwhelms ecologically-relevant patterns

50   in microbiota studies, and enables prediction of recovery time, with explicit inclusion of

51   uncertainty in assessments. We offer a step change in the development of quantitative

52   microbiota-based SMART metrics for measuring rehabilitation success. Our approach may

53   also have wider applications where restorative processes facilitate the shift of microbiota

54   towards reference states.

1. INTRODUCTION

Land degradation and transformation, with negative impacts to biodiversity and ecosystem function, are estimated to impact 75% of the Earth's land surface, and this figure is projected to rise to over 90% by 2050 (IPBES, 2018). Ecological restoration—activity that supports rehabilitation of locally representative, sustainable, biodiverse ecosystems (Gann et al., 2019)—is seen as integral to reversing these impacts, as highlighted by the UN declaration of 2021–2030 as the Decade on Ecosystem Restoration (https://www.decadeonrestoration.org/). Restoration is technically challenging and requires considerable investment, without guaranteed success (Tibbett, 2015). With large investments in restoration (e.g. BenDor et al., 2015 estimate US$9.5 billion/yr is spent in the USA alone; Menz et al., 2013 estimate US$18 billion/yr is required to restore degraded lands globally), there is a need to improve the evidence base to guide continuous improvement in restoration outcomes and to underpin future investment.

Reference ecosystems provide an important basis for establishing targets and monitoring progress of restoration activities (Gann et al., 2019) (refer to online Supplementary Materials in Appendix A, Figure S1). In post-mining contexts, best practice guidelines require formal mine completion criteria to be prescribed in a matter that is specific, measurable, achievable, relevant and time-bound (SMART) (Australian_Government, 2016; Manero et al., 2021). To-date, completion criteria have largely focussed on vegetation community variables, with typical ecological measures including alpha and beta diversity reflecting the number of different taxa and community composition, respectively. For example, targets may be set at a minimum threshold similarity to a reference community. Despite available guidance, many completion criteria are ambiguous or ill-defined, and can result in unclear standards for regulators, unrealistic expectations for stakeholders, and represent a key barrier to the relinquishment of minesites

84   (Manero et al., 2021). To help move the industry towards improved definitions of completion

85   criteria, Manero et al. (2021) suggest criteria for industry best practice, which include using

86   multiple reference sites, monitoring and corrective actions (i.e., adaptive management),

87   allowing innovation-guided completion criteria, and specific objectives and indicators.

88   Soil microbial communities (microbiota) have essential roles in organic matter

89   decomposition, soil formation, and nutrient cycling, and therefore help regulate plant

90   productivity and community dynamics (Harris, 2009). Patterns of land use, vegetation

91   communities, and soil quality each help to shape soil microbiota (Bulgarelli et al., 2013;

92   Delgado-Baquerizo et al., 2018; Turner et al., 2013). Microbiota depend on the resource and

93   energy flows associated with aboveground biota, and therefore their monitoring may help

94   indicate the impact of restoration interventions (Harris, 2009; Jiao et al., 2018; van der Heyde

95   et al., 2020).

96   The development of low-cost, high-throughput sequencing of environmental DNA

97   (eDNA) has enabled affordable, rapid and comprehensive assessment of soil microbiota; and

98   these genomic techniques are now being used widely in a restoration context (Breed et al.,

99   2019; Mohr et al., 2022). Applying recognised ecological assessment approaches to abundant

100   eDNA-based microbiota data has potential to provide a novel tool for measuring trajectories

101   and predicting time to recover towards restoration targets (Rydgren et al., 2019).

102   Chronosequence study designs, while containing limitations (Walker et al., 2010), are

103   commonly used to examine ecosystem recovery following restoration activities (Tibbett,

104   2010). However, there are few studies of soil microbiota from restoration chronosequences

105   that explicitly visualise and evaluate patterns in ecological similarity to reference data with

106   time since rehabilitation. It is customary for such studies (e.g., Fernandez Nuñez et al., 2021;

107   Jiao et al., 2018; Schmid et al., 2020) to examine patterns in microbiota composition via

108   analysis of taxonomic groups and ordination techniques which project multivariate

109   community data into lower dimensional space (e.g., 2-d plots). These popular techniques

110   often characterise the complexity and site-specificity of soil ecosystems. However, a focus on

111   measuring 'similarity to reference' may help cut through the complexity inherent to

112   microbiota data. Along these lines, van der Heyde et al. (2020) visualised temporal trends in

113   ecological similarity to reference data in post-mining rehabilitation—however, in their

114   example each rehabilitation sample was only compared to a single closest reference sample,

115   which potentially limited insight into variability and uncertainty in microbiota recovery.

116   Here we provide a proof-of-concept demonstration and detailed exploration of a new

117   complexity-reducing application of eDNA-based soil bacterial community data to assess the

118   progress of post-mining rehabilitation using three long-term (> 25 year) chronosequence case

119   studies from south-west Western Australia. Specifically, we aim to demonstrate the use of

120   chronosequence-based rehabilitation trajectories, using measures of percent similarity of

121   bacterial community structure to ecological reference sites (hereafter termed references), to

122   assess progress of soil bacterial communities towards reference states with increasing

123   rehabilitation age. We note that further work that links microbiota to other ecosystem

124   components (e.g., vegetation, fauna) is important but beyond the scope of our study.

125   Our intended audience includes microbiome researchers working in ecosystem

126   restoration, as well as restoration managers who are considering new methods to add to their

127   ecological monitoring toolkit. Our approach may also be adapted for monitoring and

128   predicting microbiota recovery toward reference states in broader contexts, including

129   microbiota-conscious urban design (Watkins et al., 2020) which represents an extension of

130   ecosystem restoration in urban areas; and microbiota-mediated human health where the

131   notion of diverse healthy reference states is well recognised (Lloyd-Price et al., 2016).

132   Due to the potential for alternative data processing options to cause varying impacts

133   on our rehabilitation trajectory assessments, we compare outcomes from a range of potential

options relevant to microbiota data analyses. For example, compositional data analysis

approaches are promoted to have greater statistical rigour compared to standard approaches

(Gloor et al., 2017); grouping bacterial taxa based on sequence similarity (i.e., varying the

resolution of operational taxonomic units, OTUs) might help manage noise associated with

microbiome data; taxonomic grouping might assist interpretation if recognised groups can be

discussed; and eliminating rare taxa (to simulate reduced sequencing depths) might allow

more cost-effective and rapid analyses. We also recognise the potential for spatial

autocorrelation—where measured outcomes are closer in value due to closer spatial

proximity—to confound the assessment of rehabilitation age in chronosequence studies that

lack appropriate spatial design and replication. Accordingly, our *a priori* research questions

were: (1) can soil bacterial community data be used to establish reference-based targets? (2)

can soil bacterial community rehabilitation trajectory data be used to predict the time to

recover to reference targets? and (3) how are these predictions of recovery influenced by

different ecological distance/similarity measures and sequence data resolution? (4)

Additionally, we conduct a preliminary, illustrative examination of spatial autocorrelation,

and trial an approach to highlight and 'correct' datasets where its influence appears

excessive. We then discuss limitations and synthesise our findings to inform future work.

2. MATERIALS AND METHODS

2.1 Data collection

We used surface soil bacterial 16S rRNA marker gene data from three case study minesites

(Figure 1; Appendix A, Tables S1–S3) from south-west Western Australia. Soil sampling

was undertaken in accordance with Australian Microbiome (AM) protocols (Bissett et al.,

2016; https://www.australianmicrobiome.com/protocols; Appendix A, Supplementary

Methods). Each minesite experiences a Mediterranean-type climate with hot, dry summers

159 and cool, wet winters. Post-mining rehabilitation activities typically involved deep-ripping,

160 prior to the 'direct return' (where possible) of subsoil and topsoil stripped from a separate pit

161 about to be mined, followed by revegetation with locally appropriate seed of diverse plant

162 communities (Tibbett, 2010). Precise soil handling and storage techniques differed between

163 the minesites and different pits within minesites. Summary information for each minesite is

164 provided below (see Appendix A, Supplementary Methods for more background information;

165 other studies in-progress will provide expanded analyses of surface and subsoil data from

166 these minesites, including additional marker gene datasets).

167   Alcoa's *Huntly* bauxite-producing minesite is approximately 100 km south-east of

168 Perth, occurring in mixed open forest with dominant overstorey species of Jarrah (*Eucalyptus*

169 *marginata*) and Marri (*Corymbia calophylla*) on lateritic, nutrient poor soils. We consider

170 Huntly data sampled in 2016, with rehabilitation ages between 2–29 years old. Huntly's 36

171 samples correspond to rehabilitation years: 1987 (n = 3), 1991 (n = 3), 1999 (n = 3), 2002 (n

172 = 3), 2008 (n = 3), 2014 (n = 3), reference (n = 18), where each reference site was paired with

173 an adjacent rehabilitation site.

174   Iluka Resource's *Eneabba* mineral-sand minesite is approximately 280 km north of

175 Perth, occurring in sandplain heath vegetation comprising low shrubland on undulating

176 infertile siliceous sandplains, predominantly featuring perennial woody species from the

177 Proteaceae, Myrtaceae, and Fabaceae families. We consider Eneabba data sampled in 2019,

178 with rehabilitation ages between 7–38 years. Eneabba's 26 samples correspond to

179 rehabilitation years: 1981 (n = 3), 1989 (n = 2), 1995 (n = 3), 2000 (n = 2), 2004 (n = 3),

180 2009 (n = 2), 2012 (n = 2), reference (n = 9).

181   South32's *Worsley* bauxite-producing minesite is located approximately 150 km south

182 of Perth, occurring in Jarrah (*Eucalyptus marginata*) forest on lateritic, nutrient poor soils.

183 We consider Worsley data sampled in 2019, with rehabilitation ages between 2–28 years old.

184   Worsley's 25 samples correspond to rehabilitation years: 1991 (n = 2), 1996 (n = 4), 1999 (n

185   = 2), 2002 (n = 2), 2005 (n = 2), 2007 (n = 1), 2011 (n = 3), 2017 (n = 3), reference (n = 6).

186   Each soil sample had physico-chemical analyses performed at CSBP Laboratories

187   (Perth, Western Australia) to quantify key soil abiotic variables as prescribed by AM

188   protocols, including soil texture, organic carbon, ammonium, potassium, sulphur, calcium,

189   pH, nitrate, phosphorous, and electrical conductivity.
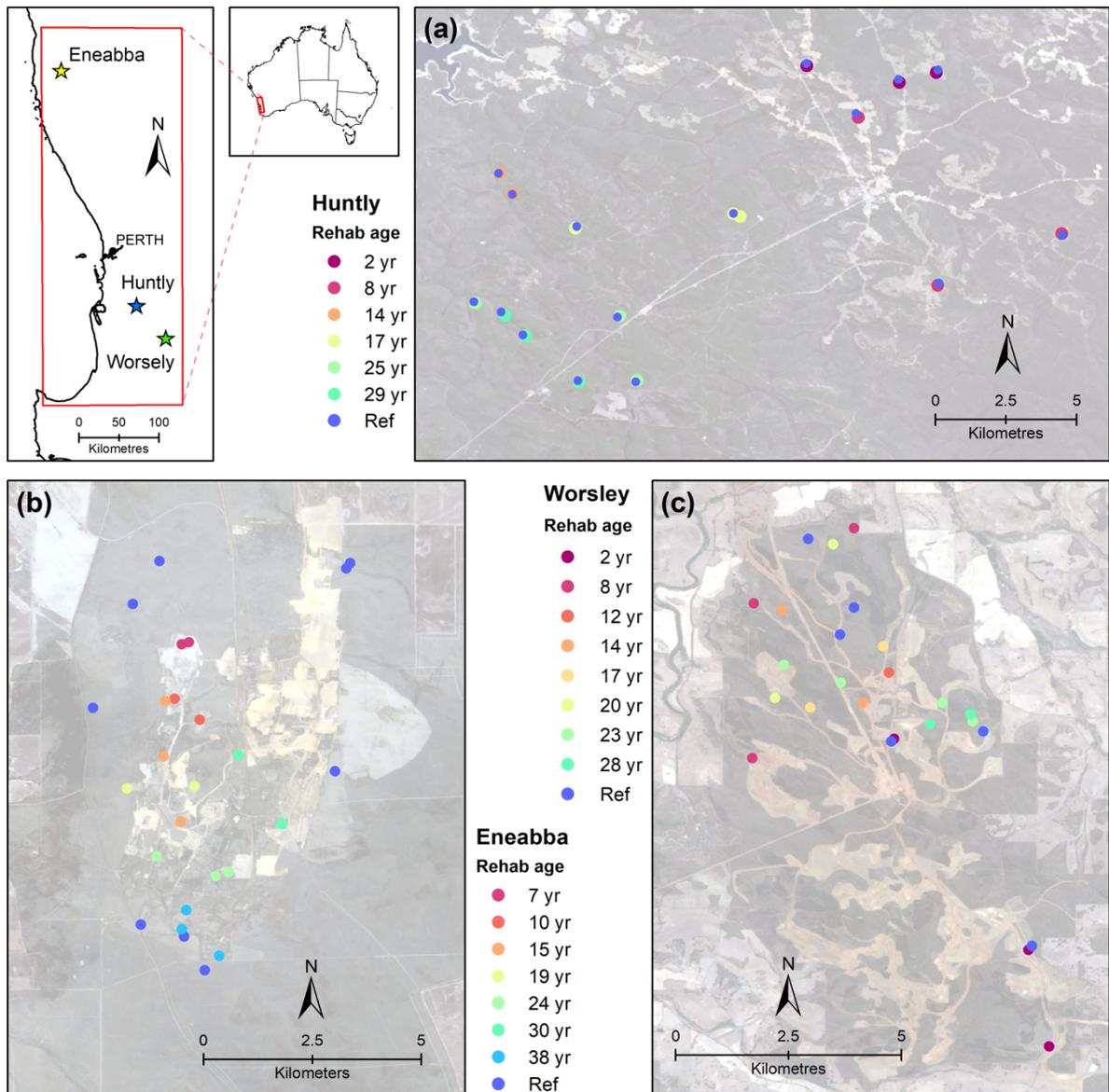
190

191   FIGURE 1. Locations of minesites and soil sampling sites: (a) Huntly, (b) Eneabba,

192   (c) Worsley. (Imagery: Sentinel-2; https://eos.com/landviewer; EOS Data Analytics, Inc.)

193

2.2 eDNA sequencing, bioinformatics, and data preparation

194

195 DNA extraction, PCR and preliminary bioinformatic analyses were undertaken in accordance

196 with AM workflows (Bissett et al., 2016; see Appendix A, Supplementary Methods). From

197 this workflow, denoised 16S rRNA gene amplicon sequence variant (ASV) level abundance

198 data were produced for all minesites. Note, in this study ASVs are equivalent to zero radius

199 OTUs (zOTUs). Further data preparation and analyses were largely undertaken in R version

200 4.0.3 (R-Core-Team, 2020) utilising the framework of the R phyloseq package (McMurdie

201 and Holmes, 2013) to manage the datasets (see Appendix A, Supplementary Methods for

202 number of sequences and ASVs studied in each minesite, initial data cleaning steps, and

203 preparation of phylogenetic trees).

204

2.3 Data visualisation and statistical analyses

205

206 We visualised the sequence depth of samples using rarefaction curves (Appendix A,

207 Figure S2). We performed exploratory data analyses to visualise ASV alpha diversity,

208 evenness, and relative abundance via heatmaps of phyla, classes, and orders in each minesite

209 (Appendix A, Supplementary Methods, Figures S3–S13). Alpha diversity and evenness were

210 based on rarefied ASV abundances (as below), while relative abundances were computed

211 using non-rarefied data. We used alternative normalisation approaches consistent with

212 common practice in the literature (Gloor et al., 2017; Weiss et al., 2017). Further exploratory

213 data analyses included preliminary visualisations of soil and landscape variables that

214 associated with the soil bacterial community samples within each minesite (see Appendix A,

215 Supplementary Methods, Supplementary Data, Figures S14–20).

216 To prepare for the computation of 'standard' ecological distance measures (as

217 described by Gloor et al., 2017; e.g. Bray-Curtis, Jaccard, UniFrac), we normalised the

218 sequence data for sampling effort by rarefying abundances of ASVs, and other taxonomic

219   levels investigated (see below), to the minimum sample sequence depth within respective

220   minesites (Huntly, n = 17,485 sequences; Eneabba, n = 10,142 sequences; Worsley, n =

221   54,122 sequences) using the *rarefy_even_depth()* function from R phyloseq.

222   To prepare 'compositional' data analysis distance measures we followed the

223   recommendations of Gloor et al. (2017) and Quinn et al. (2019), using non-rarefied data.

224   However, we took the pragmatic initial step of excluding taxa that contained zero counts in

225   more than 90% of samples within each minesite, to help limit the potential for artefactual

226   influences (as discussed later) to be introduced by the subsequent steps of zero replacement

227   and centred log ratio transformation. Then, following Quinn et al. (2019) we used the default

228   geometric Bayesian multiplicative model in the *cmultRepl()* function of the R zCompositions

229   package (Palarea-Albaladejo and Martín-Fernández, 2015) to replace zeros with small

230   numbers; before computing centred log ratio transformations using the *propr()* function from

231   the R propr package (Quinn et al., 2017). Further steps are outlined in section 2.3.1 below.

232   We examined a range of alternative qualitative and quantitative beta diversity (i.e.,

233   distance or community dissimilarity) measures which were converted to similarity, to model

234   rehabilitation trajectories and time to reach reference targets (as described further below). For

235   the minesite with the largest number of samples (Huntly), we also investigated data pre-

236   processing options of grouping by sequence similarity, taxonomic grouping, and excluding

237   rare taxa. Details of the number of samples, taxa and sequences considered for all minesites,

238   distance measures and data processing options (see below) are provided in Appendix A,

239   Table S4. Supporting data and R code used in our study are available online (see data

240   availability statement).

241

242   **2.3.1   Comparison of alternative ecological and compositional similarity measures**

243   For each minesite, we used the cleaned and rarefied ASV-level bacterial community data to

244   derive standard ecological distance matrices using distance measures commonly employed in

245   microbiota studies—i.e., Jaccard, Bray-Curtis, Unweighted UniFrac and Weighted UniFrac

246   (Lozupone et al., 2007)—via the *vegdist()* function from the R vegan package (Oksanen et

247   al., 2020). We also compared results from the Bray-Curtis measures with the compositional

248   data analysis approach from computing Aitchison distances via *vegdist()* (i.e., these were

249   derived from Euclidean distances between samples after centred log ratio transformation;

250   Gloor et al., 2017). For each minesite, Bray-Curtis distances were visualised using principal

251   coordinates analysis (PCoA) ordination, while Aitchison distances were visualised using

252   principal components analysis (PCA) (Gloor et al., 2017) (Figure 2). For the comparison

253   between Bray-Curtis and Aitchison measures at Worsley we used the spatially filtered dataset

254   which excluded the southernmost samples as described in section 2.3.6.

255   The rehabilitation trajectory analyses presented here were then derived from a subset

256   of data contained in the above distance matrices. Specifically, only pairwise distances

257   between samples and all reference samples within a minesite were considered (including

258   distances among reference samples). That is, any pairwise distances not involving a reference

259   were not included in these analyses.

260   For standard measures (i.e. Bray-Curtis, Jaccard, Weighted UniFrac and Unweighted

261   UniFrac), data were then expressed as percent similarity to reference values using (adapted

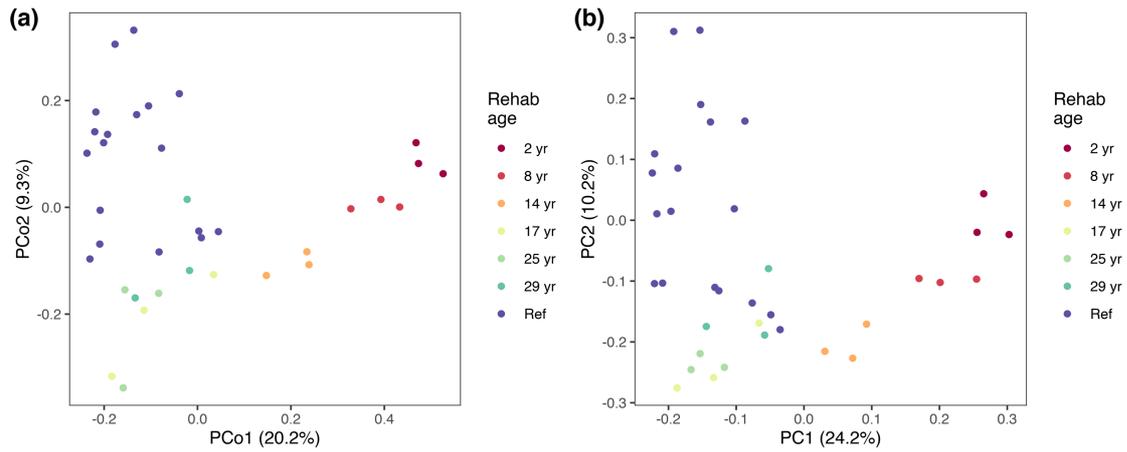262   from Legendre and Legendre, 2012):

263    $\% \text{ Similarity to reference}_{Standard\ (b/w\ sample\ i\ and\ Ref\ j)} = 100 * (1 - distance_{ij})$

264   For the compositional Aitchison measures, similarity to reference was calculated
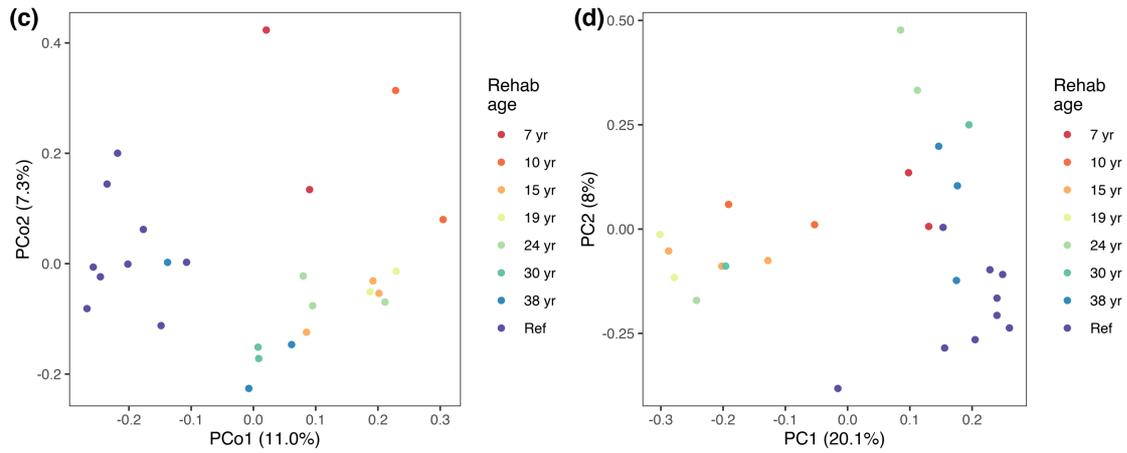
265   using (adapted from Legendre and Legendre, 2012):

266    $\% \text{ Similarity to reference}_{Aitchison\ (b/w\ sample\ i\ and\ ref\ j)} = 100 * (1 - \dfrac{distance_{ij}}{distance_{max}})$

267
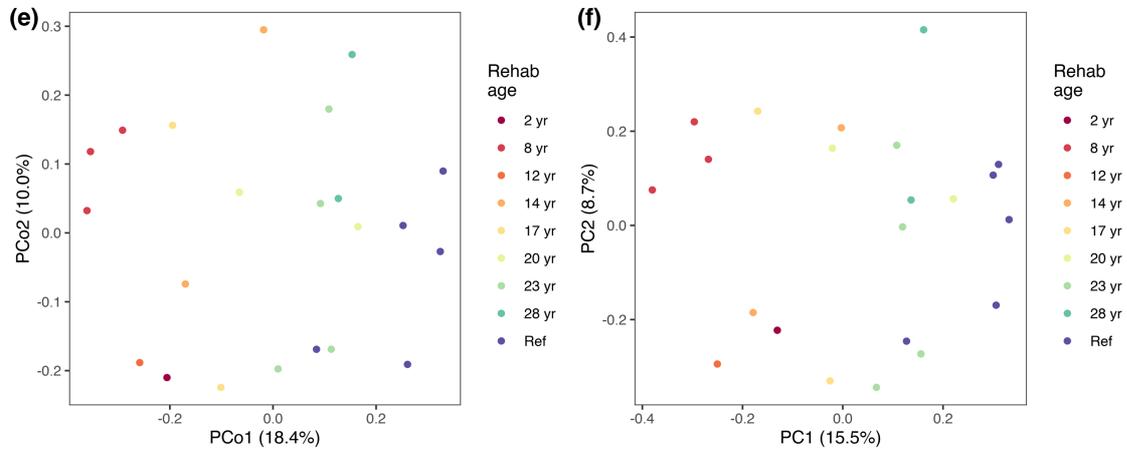
FIGURE 2. PCoA and PCA visualisations of differences in soil bacterial communities for:

Huntly (n = 36 samples) using (a) Bray-Curtis distances (30,751 ASVs; 629,460 sequences)

and (b) Aitchison distances (25,720 ASVs, 1,723,759 sequences); Eneabba (n = 26 samples)

using (c) Bray-Curtis distances (27,115 ASVs; 263,692 sequences) and (d) Aitchison

distances (24117 ASVs; 2,042,214 sequences); Worsley (excluding southernmost samples, n

277 = 22 samples) using (e) Bray-Curtis distances (53404 ASVs; 1,190,684 sequences) and (f)

278 Aitchison distances (43,598 ASVs; 1,782,724 sequences).

279

2.3.2 Grouping by sequence similarity

281 For Huntly data only, separate R phyloseq objects were generated to represent soil bacterial

282 community data with sequences clustered into 99%, 97%, 95%, and 90% identity OTUs (see

283 Appendix A, Supplementary Methods). 99% and 97% identity OTU clustering have been

284 used widely in recent years (prior to the emergence of zOTUs or ASVs), and accordingly, we

285 included OTUs with a range of clustering thresholds to examine whether consistent patterns

286 emerged. For these analyses, OTUs were formed, abundance data were rarefied, and then

287 Jaccard and Bray-Curtis distances and similarity to references were calculated.

288

2.3.3 Taxonomic grouping

290 For Huntly data only, we examined the influence of taxonomic grouping (i.e., ASV, genus,

291 family, order, class, and phylum) on the assessments of recovery. We also tested the

292 influence of discarding versus retaining (at the next available classified grouping) taxa that

293 were unclassified at each taxonomic rank, which we termed 'pruned' and 'non-pruned' data

294 respectively. Grouping was undertaken using *tax_glom()*; and in 'pruned' datasets,

295 unclassified taxa were removed using *prune_taxa()* from R phyloseq. For these analyses, taxa

296 were grouped, abundance data were rarefied, then Jaccard and Bray-Curtis distances and

297 similarity to references were calculated. Richness and evenness of sequences at the order,

298 class and phylum level were also visualised based on rarefied data and plotted together with

299 composite estimates within rehabilitation age groups from merged-sample bootstrap

300 resampling (Liddicoat et al., 2019) (B=100).

2.3.4 Excluding rare taxa

For Huntly data only, we examined the influence of excluding rare taxa, by considering all ASVs, then ASVs with >0.001 %, > 0.01%, and > 0.1% relative abundance within each minesite. For these analyses, ASVs with below the respective relative abundance threshold were removed, abundance data were rarefied, then Jaccard and Bray-Curtis distances and similarity to references were calculated.

2.3.5 Rehabilitation trajectory modelling

The progress of rehabilitation was then visualised using boxplots and logarithmic models based on the similarity to reference data. Boxplots were generated from the series of similarity to reference data on the y-axis and increasing rehabilitation age on the x-axis, concluding with reference samples (e.g., Figure 3). Testing for differences in similarities to reference at each rehabilitation age (as visualised with boxplots) was performed using the Kruskal-Wallis rank sum test, followed by post-hoc Dunn tests for multiple comparisons, with Bonferroni adjusted threshold P-values. The multiple comparison testing used default two-sided P-values and alpha = 0.05 nominal level of significance.

After observing the variation in similarity to reference values among references within each minesite (e.g., Figure 3), we defined rehabilitation targets for the purpose of this study as the median (= the central value) of among-reference similarities. This target median value varied by minesite, distance/similarity measure, and pre-processing option.

We predicted the time to reach a restoration target (= recovery time) by modelling the trend in similarity to reference with increasing rehabilitation age using bootstrapped (B = 100) logarithmic models. The median, 2.5^{th} and 97.5^{th} percentiles of predicted recovery time were evaluated. Our use of logarithmic models was consistent with the approach of Rydgren

15

326   et al. (2019), except we used similarity not distance measures. Each iteration of the bootstrap

327   involved random sampling with replacement from the available chronosequence similarity to

328   reference data, excluding outliers identified via the *boxplot()* function in base R, and

329   developing a predictive logarithmic model for similarity to reference out to a maximum

330   rehabilitation age of 500 years, or until the target was reached. Models that failed to reach the

331   target were reported with a prediction time of '>500 years'. Rectangular hyperbola and

332   negative exponential models were also trialled but were abandoned after many cases failed to

333   produce model fits. During our early analyses, we also uncovered example data that

334   highlighted a distorting influence on our trajectory (and recovery time) modelling that

335   appeared to be consistent with the application of 'direct return' soils in young rehabilitation

336   sites. Specifically, this soil material was more similar to references than older rehabilitation

337   sites. Including these samples with elevated similarity to references in the logarithmic

338   modelling appeared to bias models towards flatter, longer trajectories of recovery. Therefore,

339   to reflect the likely onset of recovery towards reference states we decided to only commence

340   logarithmic models (via our automated modelling algorithm) from the youngest rehabilitation

341   age group that had a next older group with increased median similarity to references. As

342   discussed later, this check on model commencement was designed to avoid likely distortions

343   in the modelling of recovery, in particular, due to potential biological inertia in direct return

344   soils (Janzen, 2016).

345

346   **2.3.6   Exploring spatial autocorrelation**

347   To explore the influence of spatial autocorrelation on our trajectory analyses, we produced

348   variogram-like plots (adapted from Webster and Oliver, 2007) using Bray-Curtis ecological

349   distances (between samples and references) on the y-axis, and geographic distances (between

350   samples and references) on the x-axis. Each rehabilitation age group was modelled as a

351 second-order polynomial, allowing the possible expression of curvilinear trendlines that

352 mimicked variogram-like relationships (i.e., increasing then flattening). Assuming reference

353 curves offered a natural baseline trend for spatial autocorrelation within each minesite

354 environment, we applied a 'correction' to the curvilinear trendline for each rehabilitation age

355 group by calculating the difference in mean-centred model curves (= rehabilitation age group

356 minus reference), such that 'corrected' data for rehabilitation age groups expressed the same

357 ecological distance-geographic distance curvilinear trend as seen for references (see

358 Appendix A, Supplementary Methods for further details of the rationale and approach for this

359 preliminary analysis). Rehabilitation trajectories and predicted recovery times were compared

360 between 'original' and 'corrected' data, for the Bray-Curtis similarities. For the Worsley

361 minesite, a filtered dataset, and corresponding correction, were also prepared which excluded

362 the three southernmost samples (i.e., two 2-year old samples and an adjacent reference),

363 which were geographically separate from the other Worsley samples (see Figure 1, and

364 Appendix A Table S3).

365

366 **3. RESULTS**

367 **3.1   General findings**

368 We found remarkable variability among reference samples within each minesite (Figure 3;

369 Appendix A, Table S5, Figures S21, S23–S25). Median among-reference similarities ranged

370 from <20% to >95% across all measures, and between approximately 30–40% for Bray-

371 Curtis measures, with variation depending on the specific distance measure, pre-processing

372 option, and minesite. All rehabilitation trajectory plots indicated recovery, displaying the

373 general pattern of increasing similarity to references with increasing rehabilitation age

374 (Figure 3; Appendix A, Figures S21, S23–S25), although the logarithmic models and

375 predicted recovery times varied with distance measures, pre-processing and minesite.

376

377

378
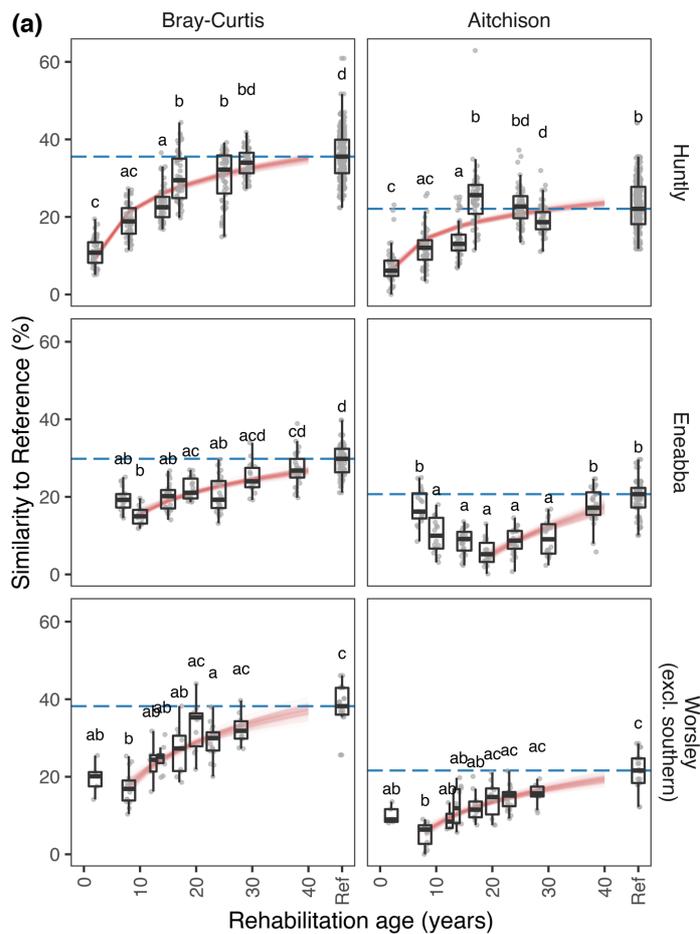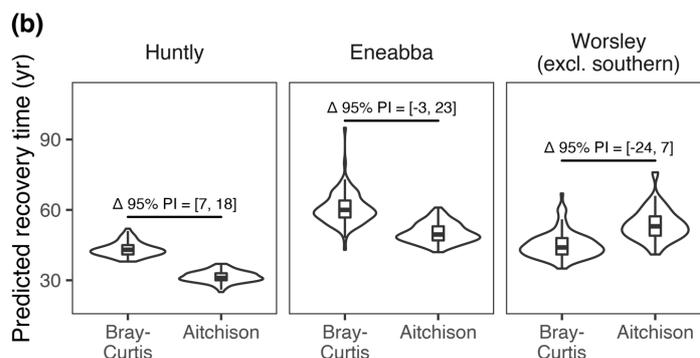
FIGURE 3. Modelled rehabilitation trajectories (a) and predicted recovery times (b) for

Huntly, Eneabba, and Worsley (excluding southernmost samples) based on surface soil

bacterial community similarity to reference data using Bray-Curtis and Aitchison measures.

Plots are derived from the same data that underpin Figure 2. In (a), blue dotted lines denote

the target median similarity among reference soils, and red lines represent logarithmic models

384   for changing similarity to reference with rehabilitation age based on bootstrap resampling and

385   modelling (B=100). Boxplots display the distribution of similarity to reference values across

386   rehabilitation ages (groups not sharing a letter are significantly different). In (b), violin plots

387   with boxplot inlays depict the distribution of recovery times from the 100 bootstrap model

388   runs. Δ 95% prediction intervals (PI) indicate whether differences in recovery times predicted

389   using alternative measures (Bray-Curtis versus Aitchison) are significantly different.

390

391   **3.2   Alternative ecological and compositional measures**

392   Despite some differences in the expression of rehabilitation trajectories using Bray-Curtis

393   versus Aitchison measures at Huntly, Eneabba, and Worsley (excluding southernmost

394   samples), these measures produced comparable predictions for recovery time within each

395   minesite (Figure 3; Appendix A, Table S6). At Huntly, predicted recovery times differed by

396   around 12 years, with a median recovery of 43 years for Bray-Curtis measures and 31 years

397   for Aitchison measures. At Eneabba, the median Bray-Curtis recovery time was 60 years,

398   while the median Aitchison recovery time was 50 years, however due to the spread of model

399   outcomes, predictions from these measures were not significantly different (i.e., Δ 95%

400   interval contains zero; Figure 3). Similarly, at Worsley (excluding southernmost samples),

401   the median Bray-Curtis recovery time was 44 years, while the median Aitchison recovery

402   time was 53 years, however predictions from these measures were not significantly different

403   (i.e., Δ 95% interval contains zero; Figure 3).

404   Among standard measures we found a general increase in similarity to reference

405   values across the ecological measures, from Jaccard (generally lowest similarities), Bray-

406   Curtis, Unweighted UniFrac, to Weighted UniFrac (generally highest similarities) (Appendix

407   A, Figure S21, Table S5). The greatest y-axis span, and therefore greatest sensitivity to detect

408   change, in similarity to reference values between the youngest rehabilitation ages and

19

409   references occurred with Bray-Curtis measures (Appendix A, Figure S21). The smallest span

410   (or flattest curves) in similarity to reference values between the youngest rehabilitation ages

411   and references occurred with Weighted UniFrac measures.

412   Except for the Unweighted Unifrac result at Huntly, Jaccard measures generally

413   returned the longest predicted recovery times, followed by reduced or similar recovery times

414   predicted using Bray-Curtis, Unweighted Unifrac and Weighted UniFrac measures

415   (Appendix A, Figure S22, Table S6). Low sample sizes (and corresponding low numbers of

416   distance measures) represent a limitation in our analysis, and the ecologically-distant samples

417   in the 17-year and 25-year rehabilitation age group at Huntly (Figure 2a) are likely

418   contributing to the reduced similarity and longer rehabilitation trajectory in Unweighted

419   UniFrac data. These 17-year and 25-year rehabilitation age group data at Huntly express

420   reduced alpha diversity and evenness compared to other samples, however reasons for this

421   are unclear (Appendix A, Figures S3–S4).

422

423   **3.3   Grouping by sequence similarity (Huntly only)**

424   Grouping by sequence similarity resulted in progressive overall shifts towards increasing

425   similarity to reference values from ASV-level (generally lowest similarities), 99%, 97%,

426   95%, to 90%-identity clustered OTUs (generally highest similarities) (Appendix A, Figure

427   S23). Predicted recovery times with more broadly clustered OTUs followed continuous and

428   seemingly predictable patterns of: (i) increasing recovery times with Jaccard measures (i.e.,

429   medians of 61 to 134 years), and (ii) decreasing to steadying recovery times with Bray-Curtis

430   measures (i.e., medians of 43 to 37 years) (Appendix A, Figure S26a, Table S6).

431

432   **3.4   Taxonomic grouping (Huntly only)**

433   Moving from ASV to genus-level data resulted in a pronounced shift towards increasing

434   similarity to reference, with similar although somewhat flatter rehabilitation trajectory curves

435   at higher taxonomic groupings (Appendix A, Figure S24). Visually, there appeared to be little

436   effect on the rehabilitation trajectory plots from pruning unclassified taxa (Appendix A,

437   Figure S24). Using Jaccard measures, moving from ASV-level to grouping at genus-level or

438   higher groupings dramatically increased predicted recovery times, compared to other

439   measures (Appendix A, Figure S26b, Table S6). Also, pruning of unclassified groups reduced

440   the smoothness or continuity in Jaccard-predicted recovery times (Appendix A, Figure S26b).

441   Using Bray-Curtis measures, we found a non-linear pattern of recovery times across the

442   taxonomic groupings, with shorter times to reach the target in genus, family, and order-level

443   groups, and longer recovery times in other groupings (Appendix A, Figure S26b; see

444   Appendix A, Figures S5–S13 for relative abundances of order, class, and phylum-level taxa

445   for each minesite). Richness and evenness of bacterial communities varied across

446   rehabilitation age groups and taxonomic groupings (e.g., data for phylum, class, and order-

447   level are shown in Appendix A, Figure S27), which may help explain the somewhat erratic

448   results from taxonomic grouping.

449

450   **3.5   Excluding rare taxa (Huntly only)**

451   Removing rare taxa to the point of retaining ASVs with >0.01% relative abundance produced

452   results from the Jaccard analysis that appeared to mimic results from the Bray-Curtis analysis

453   (Appendix A, Figure S25). When only more common ASVs with >0.1% relative abundance

454   were retained, both the Jaccard and Bray-Curtis results appeared to reflect over-simplified

455   communities, resulting in shorter predicted recovery times. However, including only ASVs

456   with >0.001% relative abundance resulted in a dataset with approximately 60% of the

457   original taxa and 95.8% of total sequences after rarefying (i.e., 17,941 compared to 30,751

458   ASVs and 603,072 compared to 629,460 sequences; Appendix A, Table S4) and produced

459   only a small increase in predicted recovery times for both Jaccard and Bray-Curtis measures

460   (Appendix A, Figure S26c, Table S6).

461

462   **3.6   Correcting for spatial autocorrelation**

463   We modelled the slope-trends of the relationships between ecological distance to references

464   and geographic distance to references, within rehabilitation age classes, for each of the

465   minesites using Bray-Curtis measures (see Appendix A, Huntly and Eneabba: Figures S28–

466   S29; Worsley: Figure 4). We also applied a 'correction' for the spatial autocorrelation, such

467   that rehabilitation age groups were adjusted to display the same ecological-geographic slope

468   trend as found in references (refer to the 'c' panels in Appendix A, Figures S28–S29; Figure

469   4). Figure 4d–f also includes the Worsley 'filtered' dataset and corresponding correction,

470   where the three southernmost geographically separate samples were excluded. Rehabilitation

471   trajectory plots, and predicted recovery times, using corrected data were compared to the

472   original uncorrected data (see Figure 5 and Appendix A, Table S6). In the case of Huntly and

473   Eneabba, only minor differences were found between original and corrected predicted

474   recovery times (Huntly: medians of 43 vs. 41 years, Δ 95% prediction interval = [1, 4];

475   Eneabba: medians of 60 vs. 56 years, Δ 95% prediction interval = [-1, 11]).

476   However, results from the Worsley data are featured because of the illustrative signal

477   we found there. Worsley displayed a strong ecological distance-geographic distance trend in

478   among-reference data indicating excessive spatial autocorrelation (note the upward sloping

479   'Ref' line in Figure 4a), and the greatest divergence of all the minesites in predicted recovery

480   times between original and corrected data (i.e., medians of 39 vs. 50 years, Δ 95% prediction

481   interval = [-49, 5]; Figure 5; Appendix A, Table S6). Notably, the spatial autocorrelation

482   correction at Worsley caused such an adjustment in similarity to reference values that the

22

483 youngest rehabilitation age group was included in the logarithmic trajectory models in the

484 corrected data, but not in the original data. However, with exclusion of the southernmost

485 Worsley samples (i.e., the filtered dataset), the signal of spatial autocorrelation disappeared

486 (i.e., absence of upward sloping lines in Figure 4d, f) and predicted recovery times for filtered

487 and filtered-corrected data displayed almost identical distributions (i.e., median recovery

488 times were equivalent at 44 years in each scenario, Δ 95% prediction interval = [-9, 9]; Figure

489 5; Appendix A, Table S6).

490
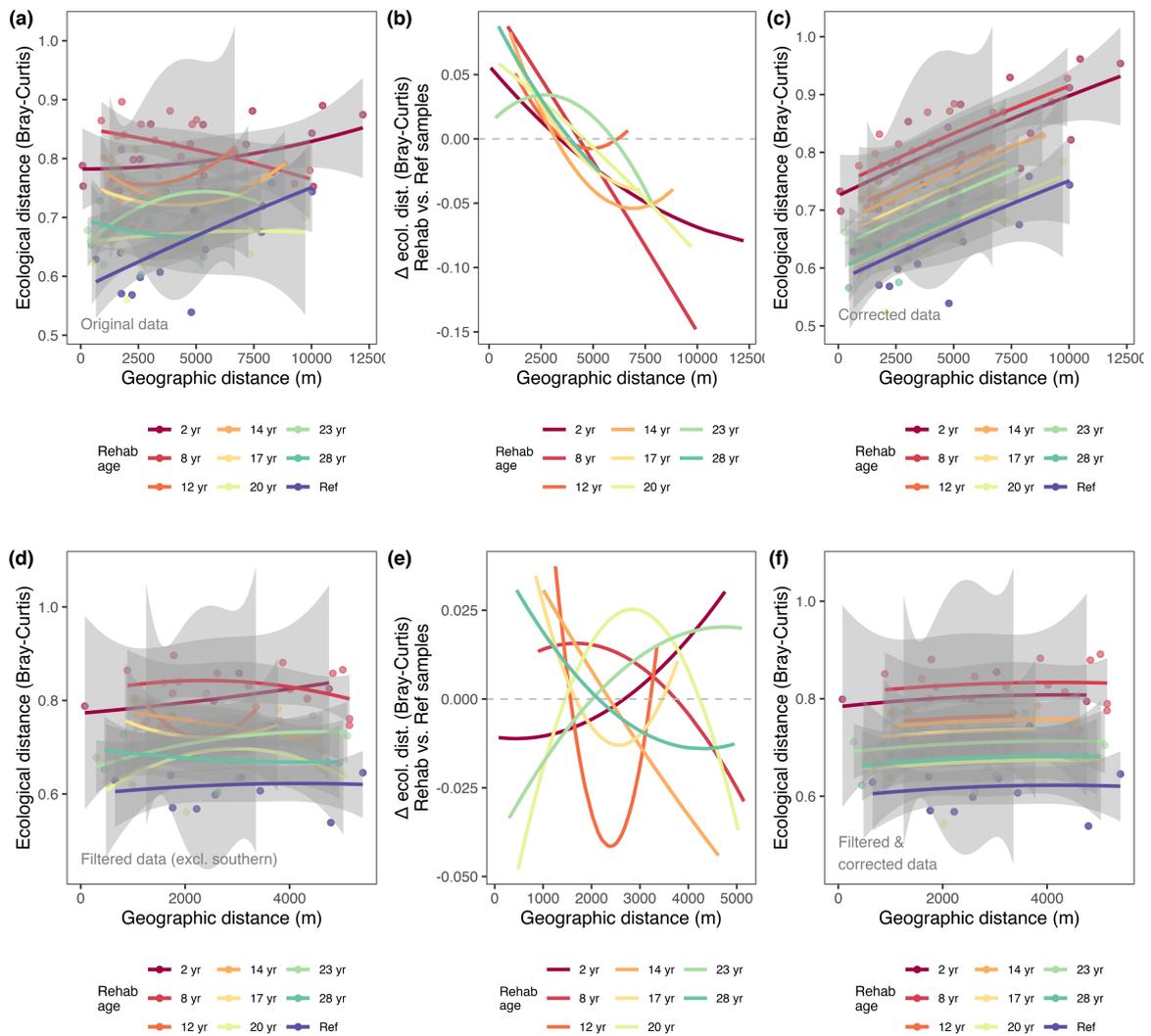
491

492

493 FIGURE 4. Exploring spatial autocorrelation in the Worsley (a–c) and filtered Worsley

494 (excluding southernmost samples) (d–f) datasets, based on Bray-Curtis distance measures.

23

495   (a, d) Ecological distance to reference versus geographic distance to reference for

496   rehabilitation age groups. (b, e) Mean-centred difference in ecological distance to reference

497   between rehabilitation age groups and among references. (c, f) Corrected ecological distance

498   to reference versus geographic distance to reference for rehabilitation age groups, to match

499   the slope-trend of ecological to geographic distances as found among references.
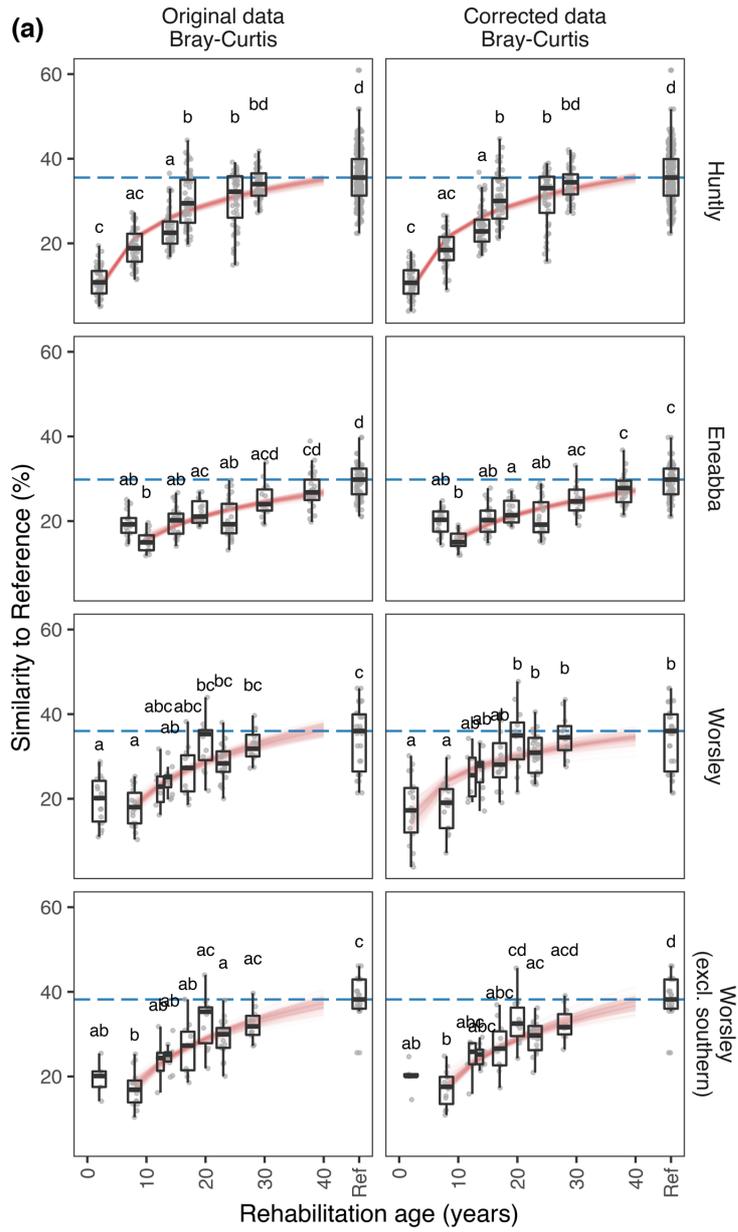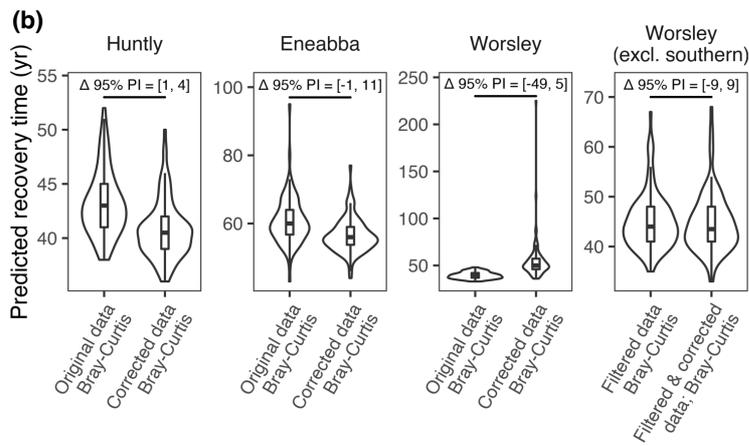
502 FIGURE 5. Modelled rehabilitation trajectories (a) and predicted recovery times (b) for

503 Huntly, Eneabba, Worsley, and Worsley (excluding southernmost samples) based on surface

504 soil bacterial community similarity to reference data using Bray-Curtis measures, with and

505 without correction for spatial autocorrelation. Other features are as described in Figure 3.

506

507 **4. DISCUSSION**

508 **4.1   Standard vs. compositional data analysis**

509 Our rehabilitation trajectory models produced comparable predictions for recovery times

510 using Bray-Curtis (standard) and Aitchison (compositional) measures. At Huntly, Eneabba,

511 and Worsley (excluding southernmost samples) median recovery times differed by around a

512 decade (i.e., 43 vs. 31 years, 60 vs. 50 years, 44 vs. 53 years respectively), however for two

513 out of three minesites the distribution of bootstrap model predicted recovery times was not

514 significantly different. We suspect that both Bray-Curtis (standard) and Aitchison

515 (compositional) measures will provide slightly different perspectives to the trajectory

516 modelling (discussed below), while neither method is perfect.

517   Compositional data analysis has been recently promoted as a more robust approach

518 for analysing microbiome datasets (Gloor et al., 2017; Quinn et al., 2019), however it is not

519 without limitations particularly for sparse datasets (containing many zeros), and where low

520 sequence counts are commonly encountered (Lovell et al., 2020). In particular, replacement

521 of zeros with small positive numbers has potential to cause distortions in data that will affect

522 the relative abundance of small counts to a greater degree than large counts (Lovell et al.,

523 2020). Distortions in data due to zero replacement are also increased where there are large

524 numbers of zeros present (Martín-Fernández et al., 2015). Therefore, our approach to exclude

525 taxa that contained zero counts in more than 90% of samples within each minesite represents

526 a compromise between losing representation of less common taxa and potentially introducing

527 spurious log ratio abundance patterns within the compositional data analysis. Following log

528 ratio analysis, only the relative information is of interest; for example, counts of 1,2,3

529 become equivalent to counts of 100, 200, 300. However, advocates of these approaches have

530 suggested that it is up to the analyst to decide whether the relative, rather than the absolute,

531 structure of the parts is of primary interest (Martín-Fernández et al., 2015). Also, the

532 replacement of absolute zeros (representing true absences; as opposed to zeros due to

533 rounding or resulting from insufficiently large samples) with small numbers is potentially

534 inappropriate (Martín-Fernández et al., 2015), and creates a theoretical challenge to

535 performing log ratio analyses on soil microbiota data from diverse environments where many

536 absolute zeros (true absences) are likely.

537

538 **4.2   Alternative standard ecological measures**

539 Bray-Curtis measures produced the greatest range in similarity values between young

540 rehabilitation and reference samples, and therefore are likely to offer the greatest sensitivity

541 to quantify the progress of recovery of soil bacterial communities towards reference states. In

542 contrast, Weighted UniFrac offered limited sensitivity to detect changes with rehabilitation

543 age (i.e., shallow trajectory curves) and may result in under-prediction of recovery times.

544 Low variation in Weighted Unifrac similarities likely reflects a level of consistency of high

545 proportions of somewhat closely related organisms across the samples. Jaccard distances

546 represent the proportion of unshared taxa out of the total number of taxa recorded in two

547 groups (Anderson et al., 2006). Unweighted UniFrac uses phylogenetic information and

548 calculates the fraction of the branch length in a phylogenetic tree that leads to descendants in

549 either, but not both, of the two communities (Lozupone et al., 2007). These qualitative

550 measures reflect the survival and presence of taxa (Jaccard) and related lineages (Unweighted

551 UniFrac), where loss of sequences may reflect extreme or limiting environmental conditions

552   (e.g., soil abiotic factors) or limited geographic distribution. Meanwhile, Bray-Curtis and

553   Weighted UniFrac measures emphasise abundant organisms. Similarity to reference generally

554   increased with increasing abundances of shared taxa for Bray-Curtis, and shared lineages of

555   related sequences for Weighted UniFrac. The quantitative measures often reflect the growth

556   or decline of certain organisms due to factors such as nutrient availability and variation in

557   environmental conditions (Lozupone et al., 2007).

558

559   **4.3   Grouping by sequence similarity**

560   Grouping near identical sequences will reduce the denominator used in calculating Jaccard

561   distances. For a given number of unshared taxa between samples, using broader OTU clusters

562   will make the proportion of unshared taxa (compared to all taxa) larger when there are a

563   smaller number of total taxa present. Our data suggest this shifting Jaccard calculation can

564   impact some samples strongly (e.g., note the 17-year age group in Appendix A, Figure S23)

565   resulting in a gradual increase in predicted recovery times with broader (reduced identity

566   threshold) OTU clusters. On the other hand, broader OTU clusters will aggregate some

567   sequences into already large groups and will tend to further emphasise abundant groups.

568   Consequently, our Bray-Curtis data suggest broader OTU clustering will make the target

569   similarity easier to reach and predicted recovery times reduced accordingly.

570

571   **4.4   Taxonomic grouping**

572   We do not recommend grouping 16S rRNA data by taxonomy to quantify recovery in soil

573   bacterial communities due to the erratic behaviour of predicted recovery times.

574

575   **4.5   Excluding rare taxa**

576 We show that filtering out of rare taxa to a limited extent (>0.001% relative sequence

577 abundance) produces a relatively small increase in predicted recovery times for both Jaccard

578 and Bray-Curtis measures. In our case, this filtering removed many ASVs but only a low

579 percentage of total sequences. Interestingly, this low level of exclusion of rare taxa does not

580 appear to moderate the assessment by producing reduced recovery times. At the low level of

581 exclusion, our analysis using rarefied data and similarity to reference measures may help

582 mitigate some of the impacts and concerns of removal of rare sequences experienced

583 elsewhere (e.g., Schloss, 2020). This raises the prospect to reduce sequencing depth, and

584 potential for shifting investment towards more robust assessments that incorporate a larger

585 number of samples with reduced sequencing depth and cost per sample.

586

587 **4.6   Influence of 'direct return' soils in young rehabilitation sites**

588 For reasons discussed here and below, we suggest it is prudent for these similarity to

589 reference trajectory assessments to exclude young rehabilitation sites with 'direct return' soils

590 that display elevated similarity to reference—as we implemented in our automated trajectory

591 modelling algorithm. In earlier preliminary work at Eneabba and Worsley, we observed that

592 the inclusion of young rehabilitation samples that were overly similar to references resulted

593 in seemingly biased, longer predictions of recovery time. The industry best practice of 'direct

594 return' of topsoil to new rehabilitation sites is based on objectives to minimise soil

595 degradation and expedite ecosystem recovery. However, our use of monotonic logarithmic

596 models applied to a data series that contains young rehabilitation sites with elevated

597 similarity to reference values, followed by older sites with reduced similarity to reference

598 values, results in the seemingly perverse outcome of a flatter, longer modelled trajectory of

599 recovery. The enhanced ecological similarity to reference in young rehabilitation sites with

600 'direct return' soils reflects a biological inertia, or temporary carryover effect, from unmined

29

601   areas where the soils originate, and confounds the relationship between soil microbiota

602   development and rehabilitation age. For 'direct return' soils, we speculate the time taken for

603   local influences to become dominant in shaping the resident microbiota may be in the order

604   of 1-10 years, varying on a case-by-case basis, e.g., due to soil factors including organic

605   matter and clay content, as well as the magnitude of environmental influences. Soil

606   microbiota will be shaped by influences including local rainfall, temperature, aspect, soil

607   water availability and transport (e.g., run-on, lateral flow), and vegetation communities via

608   plant-soil feedbacks. Existing deeper soil and substrate may also influence rehabilitation

609   surface soils via upward movement of water, nutrients, and some microbiota through

610   mechanisms including: hydraulic redistribution by plant root systems (Neumann and Cardon,

611   2012); potential microbiota uptake and transfer via xylem into the phyllosphere (Deyett and

612   Rolshausen, 2019; Fausto et al., 2018) and subsequent leaf litter; and capillary rise in heavier

613   textured soils under conditions of soil water evaporation. Other factors affecting the

614   similarity to reference of direct return soils include their source location (are they taken from

615   sites that are generally closer to other reference sites or adjacent to rehabilitation sites?), the

616   depth of fresh topsoil applied, the condition of subsurface layers (e.g., fresh vs. stockpiled),

617   and the depth and method of tillage or mixing of the soil surface and subsurface layers

618   following soil return. Our approach to automate the commencement of logarithmic models

619   once there is at least an initial increase in similarity to reference values provides an objective

620   approach to help overcome the potential model-biasing effect of biological inertia that is

621   found in some direct return soils.

622

623   **4.7   Spatial autocorrelation**

624   As observed in the Worsley data, we found signals of excessive spatial autocorrelation where

625   strong slopes were detected in plots of ecological distance to reference versus geographic

626 distance to reference, and where substantial differences were detected in the logarithmic

627 models and/or predicted recovery times between original and corrected datasets. Excluding

628 geographic outliers in the filtered Worsley analysis also removed a clear spatial

629 autocorrelation signal in the data, which indicates the importance of sampling designs. If

630 rehabilitation sites reflect environmental settings or imported soils that are overly similar or

631 dissimilar to references (i.e., different to natural background rates of spatial autocorrelation),

632 this may unduly bias predicted recovery times. Where possible, we recommend a sampling

633 approach that resembles the approach used at Huntly, where each reference site was spatially

634 paired with an adjacent rehabilitation site. This approach helps capture variation among

635 references (within a given minesite) relevant to the broader range of rehabilitation sites; and

636 provided there is adequate spatial replication and geographic outliers are avoided, then undue

637 influence from spatial autocorrelation should be avoided.

638   Our analysis of spatial autocorrelation should be viewed as introductory and

639 illustrative. For 'direct return' soils at young rehabilitation sites, our approach is deficient

640 because we do not account for their previous location. Although, we anticipate localised

641 influences would dominate the shaping of resident soil microbiota in rehabilitation sites after

642 a few years, as discussed above.

643   Plant-soil-microbiota feedbacks represent a complicating factor for disentangling

644 effects of soil abiotic condition, rehabilitation age, and residual/unexplainable spatial

645 autocorrelation in restoration chronosequence studies. This is because chronosequence

646 studies (which presume a 'space-for-time' proxy relationship between treatments and

647 outcomes) typically do not collect sufficient data to determine whether soil conditions have

648 influenced rehabilitation outcomes, plants have conditioned soils, or both situations have

649 occurred. Studies that have considered plant-soil feedbacks in restored Jarrah forest (Huntly)

650 sites have shown differential correlative effects of rehabilitated soil biotic and abiotic

651 properties (Orozco-Aceves et al., 2017). Also, plant-soil feedbacks behave differently in

652 unmined versus rehabilitated soils (Orozco-Aceves et al., 2015). Further work is required to

653 build understanding of this topic (e.g., via longitudinal studies).

654 Study designs should account for geographically variable factors that may influence

655 soil bacterial communities to build robust evidence. Microbial communities are influenced by

656 a range of often complex edaphic, physiographic, climatic and biotic factors (e.g., vegetation

657 and land use history, soil texture, available nutrients and moisture, drainage, pH, salinity,

658 sunlight; Brown et al., 2018; Delgado-Baquerizo et al., 2018; Zhu et al., 2021). The need to

659 reflect such environmental variation through choosing appropriate references is well

660 recognised by industry (Australian_Government, 2016; Manero et al., 2021).

661 Accordingly, where restoration study locations are characterised by distinct modes of

662 geographically distributed soil and landscape conditions or pre-disturbance ecosystem types

663 (e.g., uplands vs. lowlands; riparian vs. non-riparian; dune vs. swale) it would be appropriate

664 to reflect this striking contrast in reference environmental conditions and desired

665 rehabilitation outcomes by undertaking separate rehabilitation trajectory assessments for each

666 major representative target ecosystem type. The optimal distribution of each set of

667 rehabilitation and reference sites should reflect the spatial composition of major landform- or

668 post-restoration target ecosystem-types specific to each study area, and might be informed via

669 pre-existing mapping or imagery, digital elevation models, and other land resource

670 assessment tools and techniques (e.g., digital clustering of landscape types; de Bruin and

671 Stein, 1998).

672

673 **4.8   Other limitations**

674 There are important limitations in our study, in addition to those already discussed. The

675 robustness of our study would be improved with more samples per minesite to help better

676   capture minesite-wide variation. We did not consider soil microbiota patterns at depth, which

677   are also important. Also, major changes to rehabilitation practices over time will disrupt the

678   'space-for-time' substitutive modelling approach that is relied upon in chronosequence

679   studies such as ours. For any restoration chronosequence study careful sample selection is

680   required to avoid confounding factors as much as possible (Walker et al., 2010). There are

681   potential limitations in our study associated with the phylogenetic trees we used to generate

682   UniFrac distances (see Appendix A, Supplementary Methods for details). Tree-building often

683   represents a compromise between accuracy in representing phylogenetic relationships and

684   computing time, and it was beyond the scope of our study to test the sensitivity of our

685   UniFrac-based analyses to the quality of trees used. We used logarithmic models which

686   assume a monotonic recovery function, however other models that account for variable trends

687   over time, and varying success for different rehabilitation techniques or sites, may offer

688   improved estimates of recovery time. We suggest these limitations should be investigated in

689   future studies.

690

691   **5. CONCLUSIONS**

692   We provide a proof-of-concept demonstration of an innovative, chronosequence-based,

693   similarity to reference trajectory assessment method, to quantitatively track progress in soil

694   microbiota with post-mining rehabilitation. Through incorporating microbiota survey data

695   from multiple reference sites of varying character, we revealed substantial variation among

696   reference ecosystems within each minesite that can inform realistic rehabilitation targets. Our

697   method reduces the complexity associated with microbiota data and enables prediction of

698   recovery time to reach reference-based targets with explicit inclusion of uncertainty in

699   assessments. Also, the use of soil microbiota data provides another line of evidence, which in

700   conjunction with wider minesite information, could assist in the examination of potential

701 impediments to the progress of rehabilitation, thereby helping to inform adaptive

702 management. From our investigations, we recommend using ASV-level Bray-Curtis

703 similarities which appear to offer a relatively sensitive and stable basis for modelling

704 rehabilitation trajectories. We recommend wherever possible to maximise sample sizes,

705 employ spatial pairing of reference and rehabilitation sites, and to exclude geographically-

706 distant, non-representative sampling areas. We used an automated modelling routine to

707 exclude young rehabilitation sites with 'direct return' soils that displayed elevated similarity

708 to reference values, which would have biased the trajectory modelling. Further fine-tuning to

709 identify possible minor reductions in sequencing depths (eliminating some rare taxa) offers

710 promise to reduce per sample costs, enabling investment in more samples, to help deliver

711 more robust assessments. This work represents an important step towards a reduced-

712 complexity microbiota-based monitoring and evaluation framework consistent with many

713 best practice principles for setting, monitoring and managing towards mine completion

714 criteria recommended by (Manero et al., 2021). We anticipate that our approach could be

715 expanded to other eDNA sequence-based survey data (e.g., fungal ITS and eukaryote 18S

716 rRNA marker genes, functional potential from shotgun metagenomic data), and may have

717 application in wider contexts where there is interest in monitoring restorative processes that

718 facilitate a shift in microbiota towards reference states.

AUTHOR CONTRIBUTIONS

CL, SLK, MT and MFB conceived the ideas and designed the study; SLK, RJB, LCD, PB,

MPD, AG collected the data; CL, SLK, AB, MFB analysed and interpreted the data with

contributions from all authors; CL led the writing of the manuscript. All authors contributed

critically to the drafts and gave final approval for publication.

DATA AVAILABILITY STATEMENT

Data and code are available at: https://data.bioplatforms.com/organization/about/australian-

microbiome and on figshare at https://doi.org/10.25451/flinders.16920985

ORCID

Craig Liddicoat – https://orcid.org/0000-0002-4812-7524

Siegfried L. Krauss – https://orcid.org/0000-0002-7280-6324

Andrew Bissett – https://orcid.org/0000-0001-7396-1484

Ryan J. Borrett – https://orcid.org/0000-0001-8663-0844

Shawn D. Peddle – https://orcid.org/0000-0003-3464-3058

744   Mark P. Dobrowolski – http://orcid.org/0000-0001-5586-4023

745   Andrew Grigg – https://orcid.org/0000-0002-5818-2973

746   Mark Tibbett – https://orcid.org/0000-0003-0143-2190

747   Martin F. Breed – https://orcid.org/0000-0001-7810-9696

748

749

REFERENCES

Anderson, M.J., Ellingsen, K.E., McArdle, B.H., 2006. Multivariate dispersion as a measure of beta diversity. Ecology Letters 9, 683-693.

Australian_Government, 2016. Mine Rehabilitation: Leading Practice Sustainable Development Program for the Mining Industry.

BenDor, T., Lester, T.W., Livengood, A., Davis, A., Yonavjak, L., 2015. Estimating the Size and Impact of the Ecological Restoration Economy. PLOS ONE 10, e0128339.

Bissett, A., Fitzgerald, A., Meintjes, T., Mele, P.M., Reith, F., Dennis, P.G., Breed, M.F., Brown, B., Brown, M.V., Brugger, J., Byrne, M., Caddy-Retalic, S., Carmody, B., Coates, D.J., Correa, C., Ferrari, B.C., Gupta, V.V.S.R., Hamonts, K., Haslem, A., Hugenholtz, P., et_al, 2016. Introducing BASE: the Biomes of Australian Soil Environments soil microbial diversity database. GigaScience 5, 21.

Breed, M.F., Harrison, P.A., Blyth, C., Byrne, M., Gaget, V., Gellie, N.J.C., Groom, S.V.C., Hodgson, R., Mills, J.G., Prowse, T.A.A., Steane, D.A., Mohr, J.J., 2019. The potential of genomics for restoring ecosystems and biodiversity. Nature Reviews Genetics 20, 615-628.

Brown, A.G., Lespez, L., Sear, D.A., Macaire, J.-J., Houben, P., Klimek, K., Brazier, R.E., Van Oost, K., Pears, B., 2018. Natural vs anthropogenic streams in Europe: History, ecology and implications for restoration, river-rewilding and riverine ecosystem services. Earth-Science Reviews 180, 185-205.

Bulgarelli, D., Schlaeppi, K., Spaepen, S., Themaat, E.V.L.v., Schulze-Lefert, P., 2013. Structure and Functions of the Bacterial Microbiota of Plants. Annual Review of Plant Biology 64, 807-838.

de Bruin, S., Stein, A., 1998. Soil-landscape modelling using fuzzy c-means clustering of attribute data derived from a Digital Elevation Model (DEM). Geoderma 83, 17-33.

Delgado-Baquerizo, M., Reith, F., Dennis, P.G., Hamonts, K., Powell, J.R., Young, A., Singh, B.K., Bissett, A., 2018. Ecological drivers of soil microbial diversity and soil biological networks in the Southern Hemisphere. Ecology 99, 583-596.

Deyett, E., Rolshausen, P.E., 2019. Temporal Dynamics of the Sap Microbiome of Grapevine Under High Pierce's Disease Pressure. Frontiers in Plant Science 10.

Fausto, C., Mininni, A.N., Sofo, A., Crecchio, C., Scagliola, M., Dichio, B., Xiloyannis, C., 2018. Olive orchard microbiome: characterisation of bacterial communities in soil-plant compartments and their comparison between sustainable and conventional soil management systems. Plant ecology & diversity 11, 597-610.

Fernandez Nuñez, N., Maggia, L., Stenger, P.-L., Lelievre, M., Letellier, K., Gigante, S., Manez, A., Mournet, P., Ripoll, J., Carriconde, F., 2021. Potential of high-throughput eDNA sequencing of soil fungi and bacteria for monitoring ecological restoration in ultramafic substrates: The case study of the New Caledonian biodiversity hotspot. Ecological Engineering 173, 106416.

Gann, G.D., McDonald, T., Walder, B., Aronson, J., Nelson, C.R., Jonson, J., Hallett, J.G., Eisenberg, C., Guariguata, M.R., Liu, J., Hua, F., Echeverría, C., Gonzales, E., Shaw, N., Decleer, K., Dixon, K.W., 2019. International principles and standards for the practice of ecological restoration. Second edition. Restoration Ecology 27, S1-S46.

793 Gloor, G.B., Macklaim, J.M., Pawlowsky-Glahn, V., Egozcue, J.J., 2017. Microbiome
794 Datasets Are Compositional: And This Is Not Optional. Frontiers in microbiology 8, 2224-
795 2224.

796 Harris, J., 2009. Soil Microbial Communities and Restoration Ecology: Facilitators or
797 Followers? Science 325, 573-574.

798 IPBES, 2018. The IPBES assessment report on land degradation and restoration, in:
799 Montanarella, L., Scholes, R., and Brainich, A. (eds.) (Ed.), Bonn, Germany, p. 744.

800 Janzen, H.H., 2016. The Soil Remembers. Soil Science Society of America Journal 80, 1429-
801 1432.

802 Jiao, S., Chen, W., Wang, J., Du, N., Li, Q., Wei, G., 2018. Soil microbiomes with distinct
803 assemblies through vertical soil profiles drive the cycling of multiple nutrients in reforested
804 ecosystems. Microbiome 6, 146.

805 Legendre, P., Legendre, L., 2012. Chapter 7 - Ecological resemblance, in: Legendre, P.,
806 Legendre, L. (Eds.), Developments in Environmental Modelling. Elsevier, pp. 265-335.

807 Liddicoat, C., Weinstein, P., Bissett, A., Gellie, N., Mills, J., Waycott, M., Breed, M., 2019.
808 Can bacterial indicators of a grassy woodland restoration inform ecosystem assessment and
809 microbiota-mediated human health? Environment International 129, 105-117.

810 Lloyd-Price, J., Abu-Ali, G., Huttenhower, C., 2016. The healthy human microbiome.
811 Genome Medicine 8, 51.

812 Lovell, D.R., Chua, X.-Y., McGrath, A., 2020. Counts: an outstanding challenge for log-ratio
813 analysis of compositional data in the molecular biosciences. NAR Genom Bioinform 2.

814 Lozupone, C.A., Hamady, M., Kelley, S.T., Knight, R., 2007. Quantitative and qualitative
815 beta diversity measures lead to different insights into factors that structure microbial
816 communities. Applied and environmental microbiology 73, 1576-1585.

817 Manero, A., Standish, R., Young, R., 2021. Mine completion criteria defined by best-
818 practice: A global meta-analysis and Western Australian case studies. Journal of
819 Environmental Management 282, 111912.

820 Martín-Fernández, J.-A., Hron, K., Templ, M., Filzmoser, P., Palarea-Albaladejo, J., 2015.
821 Bayesian-multiplicative treatment of count zeros in compositional data sets. Statistical
822 Modelling 15, 134-158.

823 McMurdie, P.J., Holmes, S., 2013. phyloseq: An R Package for Reproducible Interactive
824 Analysis and Graphics of Microbiome Census Data. PLOS ONE 8, e61217.

825 Menz, M.H.M., Dixon, K.W., Hobbs, R.J., 2013. Hurdles and Opportunities for Landscape-
826 Scale Restoration. Science 339, 526.

827 Mohr, J., Harrison, P., Stanhope, J., Breed, M.F., 2022. Is the genomics 'cart' before the
828 restoration ecology 'horse'? Insights from qualitative interviews and trends from the
829 literature. Philosophical Transactions of the Royal Society B: Biological Sciences.

830 Neumann, R.B., Cardon, Z.G., 2012. The magnitude of hydraulic redistribution by plant
831 roots: a review and synthesis of empirical and modeling studies. New Phytologist 194, 337-
832 352.

833 Oksanen, J., Blanchet, F.G., Friendly, M., Kindt, R., Legendre, P., McGlinn, D., Minchin,
834 P.R., O'Hara, R.B., Simpson, G.L., Solymos, P., Stevens, M.H.H., Szoecs, E., Wagner, H.,
835 2020. vegan: Community Ecology Package. R package version 2.5-7.

836 Orozco-Aceves, M., Standish, R.J., Tibbett, M., 2015. Soil conditioning and plant-soil
837 feedbacks in a modified forest ecosystem are soil-context dependent. Plant and soil 390, 183-
838 194.

839 Orozco-Aceves, M., Tibbett, M., Standish, R.J., 2017. Correlation between soil development
840 and native plant growth in forest restoration after surface mining. Ecological engineering
841 106, 209-218.

842 Palarea-Albaladejo, J., Martín-Fernández, J.A., 2015. zCompositions — R package for
843 multivariate imputation of left-censored data under a compositional approach. Chemometrics
844 and Intelligent Laboratory Systems 143, 85-96.

845 Quinn, T.P., Erb, I., Gloor, G., Notredame, C., Richardson, M.F., Crowley, T.M., 2019. A
846 field guide for the compositional analysis of any-omics data. GigaScience 8.

847 Quinn, T.P., Richardson, M.F., Lovell, D., Crowley, T.M., 2017. propr: An R-package for
848 Identifying Proportionally Abundant Features Using Compositional Data Analysis. Scientific
849 Reports 7, 16252.

850 R-Core-Team, 2020. R: A language and environment for statistical computing. R Foundation
851 for Statistical Computing, Vienna, Austria.

852 Rydgren, K., Halvorsen, R., Töpper, J.P., Auestad, I., Hamre, L.N., Jongejans, E., Sulavik, J.,
853 2019. Advancing restoration ecology: A new approach to predict time to recovery. Journal of
854 Applied Ecology 56, 225-234.

855 Schloss, P.D., 2020. Removal of rare amplicon sequence variants from 16S rRNA gene
856 sequence surveys biases the interpretation of community structure data. bioRxiv,
857 2020.2012.2011.422279.

858 Schmid, C.A.O., Reichel, R., Schröder, P., Brüggemann, N., Schloter, M., 2020. 52 years of
859 ecological restoration following a major disturbance by opencast lignite mining does not
860 reassemble microbiome structures of the original arable soils. Science of The Total
861 Environment 745, 140955.

862 Tibbett, M., 2010. Large-scale mine site restoration of Australian eucalypt forests after
863 bauxite mining: soil management and ecosystem development, Ecology of Industrial
864 Pollution, pp. 309-326.

865 Tibbett, M., 2015. Mining in Ecologically Sensitive Landscapes. Victoria: CSIRO
866 Publishing, Victoria.

867 Turner, T.R., Ramakrishnan, K., Walshaw, J., Heavens, D., Alston, M., Swarbreck, D.,
868 Osbourn, A., Grant, A., Poole, P.S., 2013. Comparative metatranscriptomics reveals kingdom
869 level changes in the rhizosphere microbiome of plants. The ISME Journal 7, 2248-2258.

870 van der Heyde, M., Bunce, M., Dixon, K., Wardell-Johnson, G., White, N.E., Nevill, P.,
871 2020. Changes in soil microbial communities in post mine ecological restoration:
872 Implications for monitoring using high throughput DNA sequencing. Science of The Total
873 Environment 749, 142262.

874 Walker, L.R., Wardle, D.A., Bardgett, R.D., Clarkson, B.D., 2010. The use of
875 chronosequences in studies of ecological succession and soil development. Journal of
876 Ecology 98, 725-736.

877 Watkins, H., Robinson, J.M., Breed, M.F., Parker, B., Weinstein, P., 2020. Microbiome-
878 Inspired Green Infrastructure: A Toolkit for Multidisciplinary Landscape Design. Trends in
879 Biotechnology 38, 1305-1308.

880   Webster, R., Oliver, M.A., 2007. Geostatistics for Environmental Scientists, 2nd Edn. ed.
881   John Wiley & Sons, Ltd, West Sussex, UK.

882   Weiss, S., Xu, Z.Z., Peddada, S., Amir, A., Bittinger, K., Gonzalez, A., Lozupone, C.,
883   Zaneveld, J.R., Vázquez-Baeza, Y., Birmingham, A., Hyde, E.R., Knight, R., 2017.
884   Normalization and microbial differential abundance strategies depend upon data
885   characteristics. Microbiome 5, 27.

886   Zhu, M., Li, Y., Zhang, W., Wang, L., Wang, H., Niu, L., Hui, C., Lei, M., Wang, L., Zhang,
887   H., Yang, G., 2021. Determination of the direct and indirect effects of bend on the urban river
888   ecological heterogeneity. Environmental Research, 112166.

889